Steric effects on two inequivalent methyl internal rotations of 3,4-dimethylfluorobenzene

Julie Mélan, Safa Khemissi, Ha Vinh Lam Nguyen

Steric effects on two inequivalent methyl internal rotations of 3,4-dimethylfluorobenzene

Julie Mélan,[a] Safa Khemissi,[a] and Ha Vinh Lam Nguyen[a,b]*

[a] Laboratoire Interuniversitaire des Systèmes Atmosphériques (LISA), CNRS UMR 7583, Université Paris-Est Créteil, Université de Paris, Institut Pierre Simon Laplace, 61 avenue du Général de Gaulle, 94010 Créteil, France

[b] Institut Universitaire de France (IUF), 1 rue Descartes, 75231 Paris cedex 05, France

_____

* Corresponding author:

Ha Vinh Lam Nguyen, e-mail: lam.nguyen@lisa.ipsl.fr

Abstract

The microwave spectrum of 3,4-dimethylfluorobenzene was measured using a pulsed molecular jet Fourier transform microwave spectrometer operating in the frequency range from 2.0 to 26.5 GHz with the goal of quantifying the steric effects on the barriers to internal rotation of the two inequivalent methyl groups. Due to these torsional motions, splittings of all rotational transitions into quintets were observed and fitted with residuals close to measurement accuracy. The experimental work was supported by quantum chemical calculations, and the B3LYP-D3BJ/6-311++G(d,p) level of theory yielded accurate optimized geometry parameters to guide the assignment. The three-fold potential values of 456.19(13) cm^{-1} and 489.77(15) cm^{-1} for the methyl groups at the *meta* and *para* position, respectively, deduced from the experiments are compared with the predicted values and those of other toluene derivatives.

Graphical Abstract
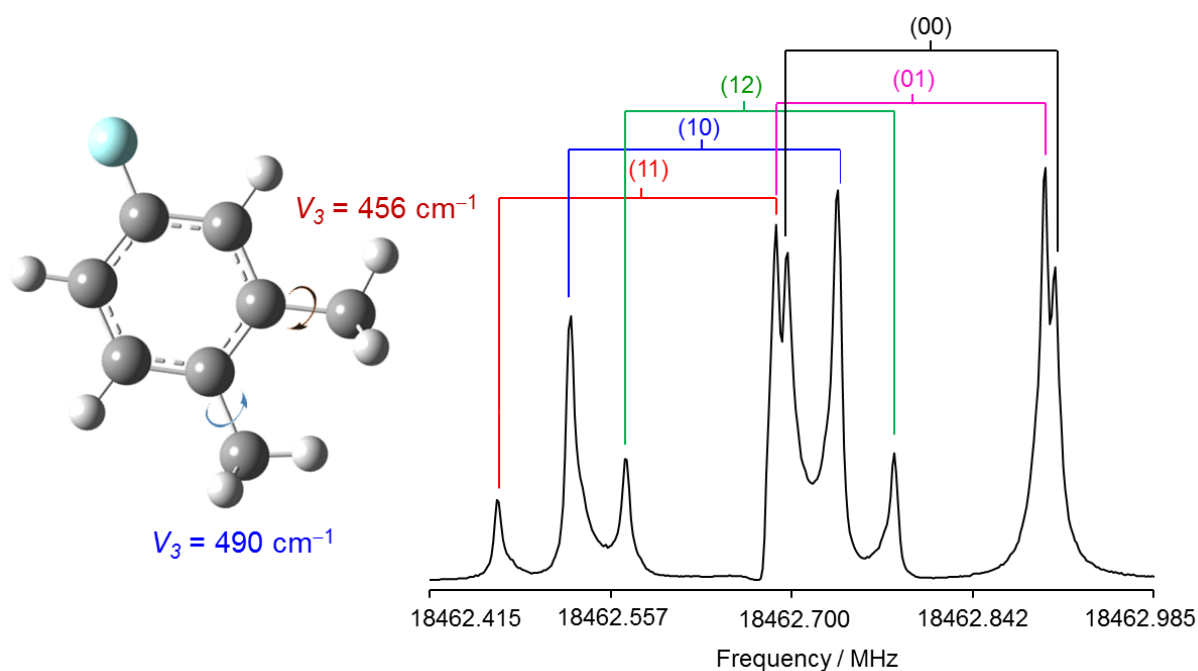
1. Introduction

The rotational spectra of many molecules show splittings arising from internal rotation of one or more methyl groups. This large amplitude motion (LAM) is a fundamental phenomenon in physical chemistry. The barrier hindering a methyl torsion varies strongly, but can be generally classified in three categories. The high-barrier-class contains molecules featuring methyl groups with torsional barrier heights larger than about 600 cm^{-1}. Ethane is the textbook example for this class with a torsional barrier of about 1000 cm^{-1} [1]. In molecules belonging to the low-barrier-class, the internal rotation of methyl groups is hindered with a barrier height lower than 200 cm^{-1}. Vinyl acetate (151.5 cm^{-1}) [2], N-ethylacetamide (73.5 cm^{-1}) [3] 3-fluorotoluene (17 cm^{-1}) [4] m- and p-methylanisole (36.6 and 49.6 cm^{-1}, respectively) [5,6], p-tolualdehyde (28.1 cm^{-1}) [7], and acetamide (25 cm^{-1}) [8], for example, fall in this class. The intermediate-barrier-class comprises of molecules with barrier heights from about 200 to 600 cm^{-1}, i.e. methyl methacrylate [9], linalool (400 cm^{-1}) [10], s-cis-acetovanillone (522 cm^{-1}) [11], N,N-diethylacetamide (517 cm^{-1}) [12], and phenylacetone (238 cm^{-1}) [13]. Some two-top molecules like acetone [14], 2,5-dimethylfuran [15], 2-acetyl-5-methylfuran [16], and 1,2-dimethylnapthalene [17] also belong to this class. The methyl torsions cause splittings up to several hundred MHz in the rotational spectrum, which can be sufficiently modeled with high accuracy by including the V_3 terms of the potential function and the orientations of the internal rotors in the Hamiltonian model.

The reason for an intermediate torsional barrier is often steric effects. In many molecules belonging to the intermediate-barrier-class, the methyl group is located in close proximity to another atom or group of the molecule. In o-xylene (**1**) [18], 3,4-dimethylanisole (**2**) [19], or 3,4-dimethylbenzaldehyde (**3**) [20], steric hindrance between the two neighboring methyl groups results in a barrier height between 400 and 550 cm^{-1} for both methyl tops. In o-substituted toluenes such as o-fluorotoluene (**5**, 227 cm^{-1}) [21], 2-chloro-4-fluorotoluene (**7**, 462 cm^{-1}) [22], o-methylanisole (**8**, 444 cm^{-1}) [23], the torsional barrier of the methyl group at the $ortho$-position of the toluene ring is intermediate. A very low torsional barrier has been observed for steric-free methyl groups, such as in propynyl group containing molecules like 2-butynol (**9**) [24], 3-pentyn-1-ol (**10**) [25], 4-hexyn-3-ol [26], tetrolyl fluoride (**11**) [27], and 2-butynoic acid (**12**) [28], where the C≡C-bond acts as a spacer that separates the methyl group from the rest of the molecule. A selection of the above mentioned molecules is illustrated in Figure 1 with molecule numbering.
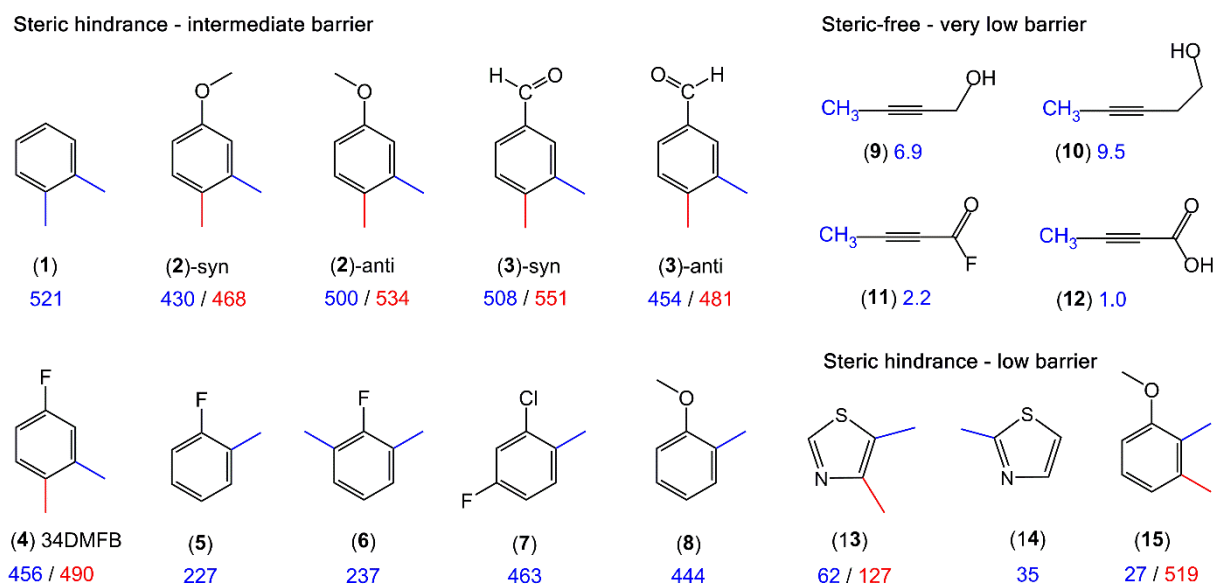
Figure 1: A selection of molecules demonstrating steric effects on methyl internal rotation: (**1**) *o*-xylene [18], (**2**) 3,4-dimethylanisole [19], (**3**) 3,4-dimethylbenzaldehyde [20], (**4**) 3,4-dimethylfluorobenzene (this work), (**5**) *o*-fluorotoluene [21], (**6**) 2,6-dimethylfluorobenzene [32], (**7**) 2-chloro-4-fluorotoluene [22], (**8**) *o*-methylanisole [23], (**9**) 2-butynol [24], (**10**) 3-pentyn-1-ol [25], (**11**) tetrolyl fluoride [27], (**12**) 2-butynoic acid [28], (**13**) 4,5-dimethylthiazole [29], (**14**) 2-methylthiazole (34.8 cm^{-1}) [31], and (**15**) 2,3-dimethylanisole [30]. The barrier heights are given in cm^{-1} and are color-coded if there are two methyl groups in the molecule.

However, steric effects cannot explain the surprisingly low torsional barriers in several cases such as 4,5-dimethylthiazole (**13**) [29], 2,3-dimethylanisole (**15**) [30], and 2-methylthiazole (**14**) [31]. In the two former molecules featuring two neighboring methyl groups, or in 2-methylthiazole where the methyl group is located between a sulfur and a nitrogen atom, one tends to assume that the methyl torsional barriers should be also intermediate between 400 and 550 cm^{-1}. This turns out to be wrong, as both methyl groups in 4,5-dimethylthiazole (**13**, 126.5 and 61.7 cm^{-1} for the 4- and 5-methyl groups, respectively) [29], the *o*-methyl group in 2,3-dimethylanisole (**15**, 26.9 cm^{-1}) [30], and the methyl group in 2-methylthiazole (**14**, 34.8 cm^{-1}) [31] all possess low to very low torsional barriers.

Recently, we started an investigation on the dimethylfluorobenzene family to study the LAMs of two methyl groups. In the first member, 2,6-dimethylfluorobenzene (**6**), the internal rotations of two methyl tops are equivalent, resulting in splittings of all rotational transitions into quartets [32]. The torsional barrier of 236.7922(21) cm^{-1} reflects well the steric effect arising from a fluorine atom located next to the methyl groups, because similar values were

found for 2-fluorotoluene (**5**) [21], n,m-difluorotoluene (n = 2, m = 3, 4, 5) [33-35], and 2,3,4- and 2,4,5-trifluorotoluene [36]. Here, we report the results for the next member, 3,4-dimethylfluorobenzene (34DMFB), where steric hindrance comes from two neighboring methyl tops. It is interesting to address the question whether the LAMs in 34DMFB are also associated with intermediate barrier heights, or it will present another exception where steric effects fail to explain the torsional barriers.

2. Quantum chemical calculations

2.1. Geometry optimizations

Geometry optimizations at three levels of theory were performed, yielding predicted rotational constants to guide the assignment. The first level was the density functional B3LYP including Grimme's dispersion correction with Becke-Johnson damping (B3LYP-D3BJ) [37] in combination with Pople's basis set 6-311++G(d,p). Calculations at this level have given predicted equilibrium rotational constants B_e which matched almost exactly the experimentally deduced rotational constants for 2,6-dimethylfluorobenzene [32]. For comparison, optimizations were also carried out at the *ab initio* MP2/6-311++G(d,p) level of theory, a level which yielded satisfactory results for many molecules of different classes of compounds in the literature [38-42]. Finally, we performed calculations at the MP2/6-31G(d,p) level, because it has provided rotational constants with values close to the experimental ones for many molecules containing a phenyl ring [43-45]. The predicted B_e constants and dipole moment components are collected in Table 1.

Figure 2 illustrates the optimized geometry of the only conformer of 34DMFB. The nuclear coordinates in the inertial principal axis system can be found in Table S-1 of the Supplementary Material. The rotational constants B_0 of the vibrational ground state were obtained by anharmonic frequency calculations at the B3LYP-D3BJ/6-311++G(d,p) and the MP2/6-311++G(d,p) levels. Subsequently, we redid the geometry optimizations at various levels of theory, using in addition to the B3LYP and the MP2 methods Truhlar's M06-2X and the coupled cluster (CCSD) methods to find other alternatives for method-basis set combinations suitable to guide the spectral assignments of molecules related to 34DMFB. The results are collected in Table S-2 in the Supplementary Material. The *Gaussian 16* program package was used for all calculations.
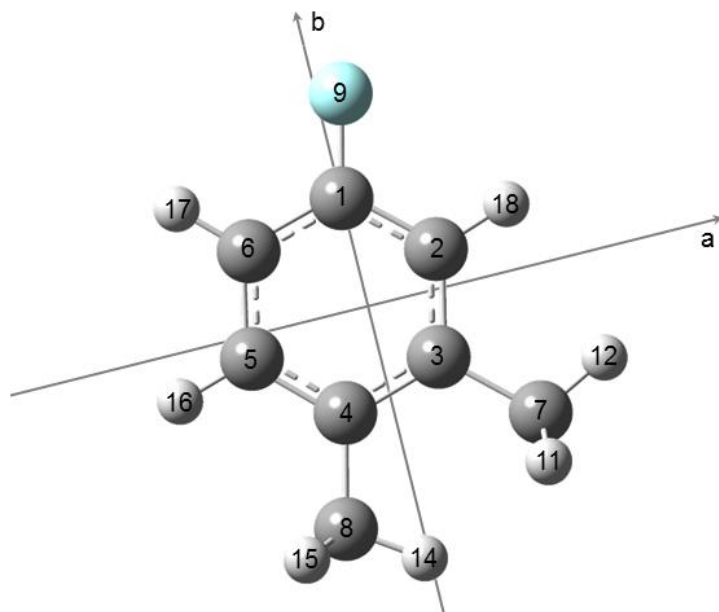
Figure 2: The molecular geometry of 34DMFB optimized at the B3LYP-D3BJ/6-311++G(d,p) level of theory. The hydrogen atoms are white, the carbon atoms grey, and the fluorine atom is light blue.

Table 1: Equilibrium B_e and vibrational ground state B_0 rotational constants (in MHz), dipole moment components (in D), and barriers to internal rotation of the two methyl groups of 34DMFB.

	B3LYP-D3BJ	MP2/6-311++G(d,p)	MP2/6-31G(d,p)
A_e	2995.4	2983.0	2992.6
B_e	1270.3	1264.8	1268.2
C_e	901.9	898.1	900.6
A_0	2963.5	2948.2	–[a]
B_0	1263.9	1257.8	–[a]
C_0	896.0	891.9	–[a]
μ_a	2.43	2.30	1.96
μ_b	−0.16	−0.16	−0.15
μ_c	0.00	0.00	0.00
$V_3(m)$[b]	416.0	401.9	410.3
$V_3(p)$[b]	445.9	436.4	434.6
$V_3^{TS}(m)$[c]	388.7	508.5	412.6
$V_3^{TS}(p)$[c]	408.7	472.5	428.2

[a] Anharmonic frequency calculations did not converge at this level of theory.

[b] Effective V_3 potential term for the *meta*- and *para*-methyl group obtained by parameterizing the energy data points with a one-dimensional Fourier expansion.

[c] Barrier height obtained from optimizations to a transition state.

2.2. Methyl internal rotations

The energy potentials describing the two methyl torsions were calculated at the B3LYP-D3BJ/6-311++G(d,p), MP2/6-31G(d,p), and MP2/6-311++G(d,p) levels of theory by varying the dihedral angles $\alpha_1 = \angle(C_2,C_3,C_7,H_{12})$ and $\alpha_2 = \angle(C_3,C_4,C_8,H_{14})$ in $10°$ steps while all other molecular parameters were optimized. Three-fold potentials were obtained, where higher V_{3n} contributions can be neglected. The values of the predicted effective V_3 potential term are 416.0 (B3LYP-D3BJ), 410.3 (MP2/6-31G(d,p)), and 401.9 cm^{-1} (MP2/6-311++G(d,p)) for the *meta* methyl group. The respective values for the *para* methyl group are 445.9, 434.6, and 436.4 cm^{-1}. In addition, we performed geometry optimizations to a first-order transition state using the Berny algorithm for comparison [46]. The results are summarized in Table 1. The torsional barriers are thus intermediate for both methyl groups. We expect that each rotational transition of 34DMFB splits into five torsional components called the $(\sigma_1\sigma_2) = (00)$, (01), (10), (11), and (12) species [19]. σ_1 refers to the *meta* and σ_2 to the *para* methyl group.

The coupling between the two inequivalent methyl torsions was explored by a two-dimensional potential energy surface (2D-PES) depending on the two dihedral angles α_1 and α_2. They were varied in a grid of $10°$, and all other structural parameters were optimized at the B3LYP-D3BJ/6-311++G(d,p) level of theory. The potential energy points were parametrized with a 2D Fourier expansion:

$$V(\alpha) = -410.26342\ Hartree + \frac{450.2\ cm^{-1}}{2} cos(3\alpha_1) - \frac{476.8\ cm^{-1}}{2} cos(3\alpha_2) - 15.3\ cm^{-1} \cdot$$
$$cos(3\alpha_1)cos(3\alpha_2). \hspace{4cm} (1)$$

Using the Fourier coefficients, the PES was drawn as a color contour plot given in Figure 3. As can be recognized from the values of the Fourier coefficients given in Eq. (1), the coupling term $cos(3\alpha_1)cos(3\alpha_2)$ between the two methyl torsions is less than 7% of the V_3 potential terms. The 2D-PES was redone at the MP2/6-31G(d,p) and MP2/6-311++G(d,p) levels and illustrated in Figure S-1 of the Supplementary Material. The results confirmed the conclusion drawn from Figure 3 and Eq. (1).
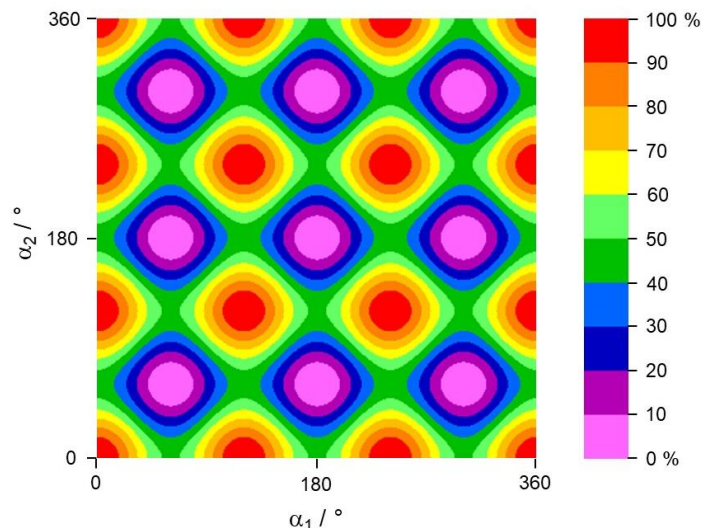
Figure 3: The potential energy surface of 34DMFB obtained by varying the dihedral angles $\alpha_1 = \angle(C_4,C_3,C_7,H_{12})$ and $\alpha_2 = \angle(C_5,C_4,C_8,H_{14})$ in a grid of 10° while all other geometry parameters were optimized at the B3LYP-D3BJ/6-311++G(d,p) level of theory. The numbers in the color code indicate the energy in percent with respect to the lowest energy conformations at $E_{min} = -410.2654622$ Hartree (0%) and the highest energy conformations at $E_{max} = -410.2612507$ Hartree (100%).

3. Microwave spectroscopy

3.1. Measurements

The microwave spectrum of 34DMFB was recorded in the frequency range from 2 to 26.5 GHz using a pulsed molecular jet Fourier transform spectrometer with a coaxially oriented beam-resonator arrangement (COBRA) [47]. A few drops of 34DMFB were put on a piece of a pipe cleaner placed in front of the nozzle, and helium as carrier gas was passed over the sample at a stagnation pressure of 2 bars. For all survey spectra, overlapping high-resolution spectra with 30 co-added decays per each spectrum were automatically recorded at a step width of 0.25 MHz.

In the high-resolution spectra, each line appears as doublets arising from the Doppler effect. For isolated lines, the instrumental accuracy is estimated to be approximately 2 kHz [48]. For 34DMFB, line broadening is observed for most of the lines, which might arise from unresolved internal rotation splittings, especially those of the (00) and (01) species, as well as the spin-spin and spin-rotation coupling of the hydrogen atoms. Therefore, the estimated measurement accuracy is 4 kHz. A typical spectrum is illustrated in Figure 4.
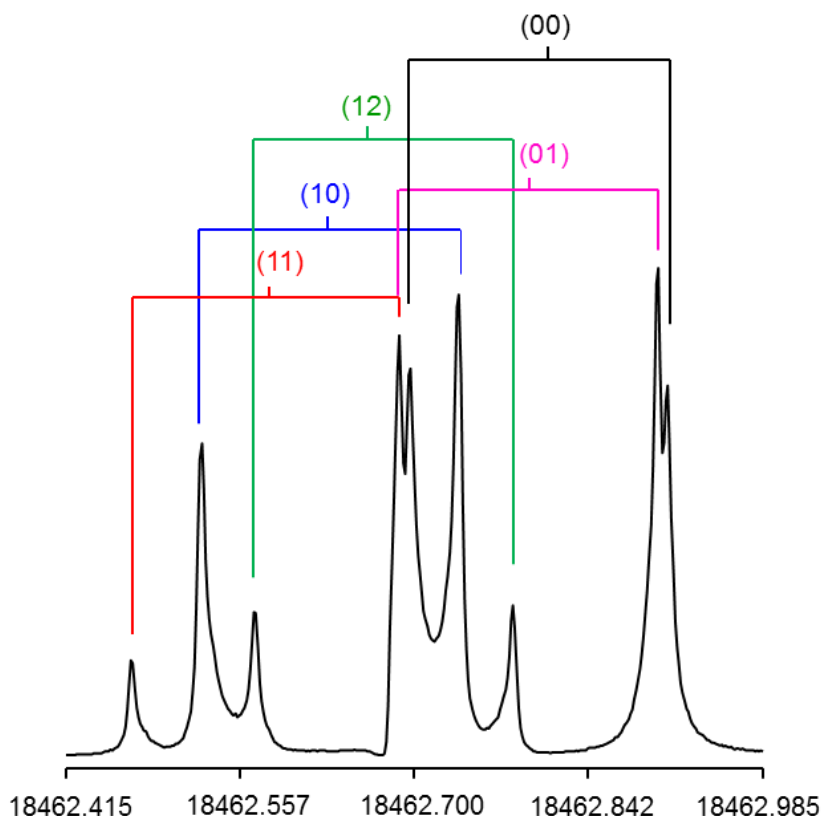
Figure 4: A spectrum of the $8_{35} \leftarrow 7_{34}$ transition of 34DMFB recorded at high resolution which splits into the (00), (01), (10), (11), and (12) torsional species. The frequencies are given in MHz. The Doppler doublets are marked by brackets.

3.2. Spectral assignment

The predicted dipole moment components given in Table 1 have shown that the component along the *a*-axis of the molecule has the largest value. The *b*-component is very small, and the *c*-component is zero. Therefore, we only expect a pure *a*-type microwave spectrum. Transitions of *b*-type, if still observable, should be weak. Using the rotation constants calculated at the B3LYP-D3BJ/6-311++G(d,p) level, we predicted the spectrum of the rigid rotor using the *XIAM* code [49]. We first searched for the *a*-type $5_{05} \leftarrow 4_{04}$ transition predicted at 10011 MHz and recorded a survey spectrum starting at 10000 MHz, where we found an intense line at 10030 MHz. This has confirmed the reliability of the calculated rotational constants. Therefore, for the next transition $5_{14} \leftarrow 4_{13}$ predicted at 11480 MHz, we recorded a small scan portion from 11470 to 11515 MHz and found the line at 11513 MHz. A further scan from 9725 to 9762 to search for the $5_{15} \leftarrow 4_{14}$ transition predicted at 9738 MHz confirmed the assignment, where we found an intense line at 9760 MHz. Further transitions could be observed easily afterwards. At this stage, we did not consider the internal rotation of the two methyl groups.

To take into account the torsional motions and model the spectrum, the V_3 potential terms of the two methyl rotors predicted at the B3LYP-D3BJ/6-311++G(d,p) level were used in the program *XIAM*. The angles $\angle(i,a)$ between the a principal axis of the molecule and the axes of the internal rotors were taken from the geometry optimized at the same level. The torsional components (00), (01), (10), (11), and (12) of the quintets could be assigned straightforwardly. As the b-dipole moment component is very low and b-type transitions are weak, it is not possible to check the assignment by combination difference loops. As an alternative, we used the *SFLAMS* program (Separately Fitting of Large Amplitude Motion Species) [50] to fit each torsional species separately. The results are shown in Table 2. For the (00) state, a semi-rigid rotor model consisting of only the rotational and quartic centrifugal distortion constants is sufficient. For the (01) and (10) species, the odd power parameter q (also called D_a in the literature), multiplying the $\mathbf{P_a}$ operator, is needed in addition. For the (11) and (12) species, the fit requires also the q_J and r (sometimes called D_b), multiplying $\mathbf{P^2P_a}$ and $\mathbf{P_b}$, respectively. The standard deviations obtained for all these fits are very close to the measurement accuracy and confirm the correct assignment.

A total of 404 lines were included in the program *XIAM* and fitted to a standard deviation of 3.9 kHz by using only the three rotational constants, four quartic centrifugal constants as well as the two V_3 terms and the two angles $\angle(i,a)$. The obtained molecular parameters are collected in Table 3. The frequency list of all fitted transitions is given in Table S-3 of the Supplementary Material

Table 2: Molecular parameters used for the *SFLAMS* fits of the (00), (01), (10), (11), and (12) species.

Par.[a]	Unit	Fit (00)	Fit (01)	Fit (10)	Fit (11)	Fit (12)
A	MHz	2985.6742(19)	2985.5975(24)	2985.6261(25)	2985.5486(22)	2985.5541(27)
B	MHz	1272.83342(13)	1272.83236(17)	1272.82150(19)	1272.81990(16)	1272.82019(19)
C	MHz	902.42696(11)	902.42702(13)	902.42726(14)	902.42733(13)	902.42702(14)
D_J	kHz	0.02287(47)	0. 02360(64)	0.02529(67)	0.02386(55)	0.02473(65)
D_{JK}	kHz	0.0651(24)	0.0646(30)	0.0606(32)	0.0665(28)	0.0545(34)
d_1	kHz	0.00666(33)	0.00733(43)	0.00749(56	0.00680(39)	0.00771(43)
q	MHz		2.3542(43)	2.2714(47)	4.62152(95)	–0.0458(11)
q_J	kHz				–0.141(12)	
r	MHz					2.14(28)
N^{b}		89	76	76	88	75
σ^{c}	kHz	3.4	4.2	4.3	3.9	4.2

[a] All parameters refer to the principal axis system. Watson's S reduction in the I$^{\text{r}}$ representation was used.
[b] Number of lines.
[c] Standard deviation of the fit.

Table 3: Molecular parameters of 34DMFB as obtained with the *XIAM* program. Rotor 1 and 2 refer to the methyl group at the *meta* and *para* positions, respectively.

Par.[a]	Unit	Fit *XIAM*	Calc.[b]
A	MHz	2985.5867(12)	2995.415
B	MHz	1272.832256(78)	1270.292
C	MHz	902.419451(61)	901.931
D_J	kHz	0.02362(26)	0.021413
D_{JK}	kHz	0.0671(14)	0.072587
d_1	kHz	–0.00818(22)	–0.007341
d_2	kHz	–0.00151(17)	–0.001501
$V_{3,1}$	cm^{-1}	456.19(13)	416.0
$V_{3,2}$	cm^{-1}	489.77(15)	445.9
$\angle(i_1,a)$	°	49.153(69)	47.81
$\angle(i_1,b)^c$	°	40.846(69)	42.18
$\angle(i_1,c)$	°	90.00[d]	90.00
$\angle(i_2,a)$	°	342.58(26)	346.39
$\angle(i_2,b)^c$	°	72.58(26)	76.39
$\angle(i_2,c)$	°	90.00[d]	90.00
N^e		404	
σ^f	kHz	3.9	

[a] All parameters refer to the main axis system. Watson's S reduction in the I^r representation was used.
[b] Calculated at the B3LYP-D3BJ/6-311++G(d,p) level. The predicted value of D_K is 0.353127 kHz.
[c] Derived from $\angle(i,a)$.
[d] Fixed due to symmetry.
[e] Number of lines.
[f] Standard deviation of the fit.

4. Results and discussion

Using the *XIAM* program, 404 torsional transitions observed in the microwave spectrum of 34DMFB were fitted with a standard deviation of 3.9 kHz, within the measurement accuracy. The rotational constants were deduced with great precision. Quartic centrifugal distortion constants, except D_K due to the observation of only *a*-type transitions, could also be well-determined.

The rotation constants obtained by quantum chemical calculations agree with the experimental ones (see Tables 1 and 3). The values of the rotation constants predicted by different combinations of methods and basis set given in Table S-2 of the Supplementary Material are in general close to the experimentally deduced values with deviations not exceeding 2%. Comparing with the results found for 2,6-dimethylfluorobenzene [32], where

the B3LYP-D3BJ/6-311++G(d,p) level of theory yielded equilibrium rotational constants B_e in almost exact agreement with the B_0 experimental ones in the vibrational ground state, we found that the agreement is also very satisfactory in the case of 34DMFB. Therefore, the B3LYP-D3BJ/6-311++G(d,p) level is recommended for other isomers of the dimethylfluorobenzene family and their derivatives. Other levels such as the MP2, B3LYP-D3, and B3LYP-D3BJ method in combination with the (d,p) polarization function, or the B3LYP-D3(BJ)/(aug)-cc-pVDZ levels also yielded very reliable results for the rotational constants to guide the spectral assignment.

To consider the two methyl internal rotations, only the V_3 potentials and the angles between the internal rotor axes and the principal a-axis were fitted. Due to the strong correlation with V_3, the internal rotational constant F_0 was set at 158 GHz, a value often found for methyl groups, which is also obtained when this parameter is floated. No coupling terms are required in the Hamiltonian to achieve a satisfactory fit. The torsional barriers of 456.19(13) cm^{-1} and 489.77(15) cm^{-1} obtained for the methyl group at the *meta-* and *para-*positions, respectively, are very similar. These intermediate values are very close to those found for 3,4-dimethylanisole (**2**) [19] and 3,4-dimethylbenzaldehyde (**3**) [20], confirming the effects of steric hindrance between two neighboring methyl groups on the methyl torsional barriers of 34DMFB. This means that unlike the cases of 4,5-dimethylthiazole (**13**) [29] and 2,3-dimethylanisole (**15**) [30], 34DMFB represents a normal case where steric effects can explain the barrier height of the methyl torsion. A comparison with the value of 236.7922(21) cm^{-1} of two equivalent methyl groups in 2,6-dimethylfluorobenzene (**6**) [32] shows that a methyl group close to a small fluorine atom undergoes internal rotation with a lower hindering barrier than that in close proximity of the bulkier methyl group. The barrier to internal rotation of the *meta-*methyl group is lower than that of the *para-*one, as also observed for 3,4-dimethylanisole (**2**) [19] and 3,4-dimethylbenzaldehyde (**3**) [20]. This difference can no longer be explained by steric effects, showing that the methyl groups are also sensitive to electronic surrounding. However, electrostatic effects are much more difficult to explore and more investigations are required to understand them.

5. Conclusion

The microwave spectrum of 34DMFB has been successfully assigned with support from quantum chemistry. Due to the internal rotation of two inequivalent methyl groups, all rotational transitions split into quintets. Using the program *SFLAMS*, the assignments were

checked by fitting separately each of the five torsional species before modeling the transition frequencies in a global fit using the program *XIAM*, which yielded a standard deviation of 3.9 kHz, within the measurement accuracy. Results from quantum chemical calculations have shown that the B3LYP-D3BJ/6-311++G(d,p) level predicts reliable rotational constants to guide the spectral assignment, but other levels such as the MP2, B3LYP-D3, and B3LYP-D3BJ method in combination with the (d,p) polarization function, or the B3LYP-D3(BJ)/(aug)-cc-pVDZ also succeed. Steric effects occurring from the adjacent positions of two methyl groups strongly influence the methyl torsional barriers.

Supplementary material

See supplementary material for the Cartesian coordinates, basis set variation, potential energy surfaces, and frequency lists.

References

[1] R. M. Pitzer, Acc. Chem. Res. 16 (1983) 207.

[2] H. V. L. Nguyen, A. Jabri, V. Van, W. Stahl, J. Phys. Chem. A 118 (2014) 12130.

[3] R. Kannengießer, M. J. Lach, W. Stahl, H. V. L. Nguyen, ChemPhysChem 16 (2015) 1906.

[4] K. P. R. Nair, S. Herbers, H.V.L. Nguyen, J.-U. Grabow, Spectro. Chim. Acta A 242 (2020) 118709.

[5] L. Ferres, W. Stahl, H. V. L. Nguyen, J. Chem. Phys. 148 (2018) 124304.

[6] L. Ferres, W. Stahl, I. Kleiner, H. V. L. Nguyen, J. Mol. Spectrosc. 343 (2018) 44.

[7] H. Saal, J.-U. Grabow, A.R. Hight Walker, J.T. Hougen, I. Kleiner, W. Caminati, J. Mol. Spectrosc. 351 (2018) 55.

[8] V. V. Ilyushin, E. A. Alekseev, S. F. Dyubko, I. Kleiner, J. T. Hougen, J. Mol. Spectrosc. 227 (2004) 115.

[9] S. Herbers, D. Wachsmuth, D. A. Obenchain, J.-U. Grabow, J. Mol. Spectrosc. 343 (2018) 96.

[10] H. V. L. Nguyen, H. Mouhib, S. Klahm, W. Stahl, I. Kleiner, Phys. Chem. Chem. Phys. 15 (2013) 10012.

[11] E. J. Cocinero, F. J. Basterretxea, P. Écija, A. Lesarri, J. A. Fernández, F. Castaño, Phys. Chem. Chem. Phys. 13 (2011) 13310.

[12] R. Kannengießer, S. Klahm, H. V. L. Nguyen, A. Lüchow, W. Stahl, J. Chem. Phys. 141, (2014) 204308.

[13 M. J. Tubergen, R. J. Lavrich, D. F. Plusquellic, R. D. Suenram, J. Phys. Chem. A 110 (2006) 13188.

[14] P. Groner, S. Albert, E. Herbst, F. C. De Lucia, F. J. Lovas, B. J. Drouin, J. C. Pearson, J. Astrophys. 142 (2002) 145.

[15] V. Van, J. Bruckhuisen, W. Stahl, V. Ilyushin, H. V. L. Nguyen, J. Mol. Spectrosc. 343 (2018) 121.

[16] V. Van, W. Stahl, H.V.L. Nguyen, ChemPhysChem 17 (2016) 3223.

[17] E. G. Schnitzler, B. L. M. Zenchyzen, W. Jäger, J. Astrophys. 805 (2015) 141.

[18] H. D. Rudolph, K. Walzer, I. Krutzik, J. Mol. Spectrosc. 47 (1973) 314.

[19] L. Ferres, J. Cheung, W. Stahl, H.V.L. Nguyen, J. Phys. Chem. A 123 (2019) 3497.

[20] M. Tudorie, I. Kleiner, M. Jahn, J.-U. Grabow, M. Goubet, O. Pirali, J. Phys. Chem. A. 117 (2013) 13636.

[21] S. Jacobsen, U. Andresen, H. Mäder, Struct. Chem. 14 (2003) 217.

[22] K. P. R. Nair, S. Herbers, W. C. Bailey, D. A. Obenchain, A. Lesarri, J.-U. Grabow, H. V. L. Nguyen, Spectrochim. Acta A 247 (2020) 119120.

[23] L. Ferres, H. Mouhib, W. Stahl, H. V. L. Nguyen, ChemPhysChem 18 (2017) 1855.

[24] R. Subramanian, S. E. Novick, R. K. Bohn, J. Mol. Spectrosc. 222 (2003) 57.

[25] K. Eibl, R. Kannengießer, W. Stahl, H. V. L. Nguyen, I. Kleiner, Mol. Phys. 114 (2016) 3483.

[26] K. Eibl, W. Stahl, I. Kleiner, H. V. L. Nguyen, J. Chem. Phys. 149 (2018) 144306.

[27] V. M. Stolwijk, B. P. van Eijck, J. Mol. Spectrosc. 124 (1987) 92.

[28] V. Ilyushin, R. Rizzato, L. Evangelisti, G. Feng, A. Maris, S. Melandri, W. Caminati, J. Mol. Spectrosc. 267 (2011) 186.

[29] V. Van, T. Nguyen, W. Stahl, H. V. L. Nguyen, I. Kleiner, J. Mol. Struct. 1207 (2020) 127787.

[30] L. Ferres, K.-N. Truong, W. Stahl, H. V. L. Nguyen, ChemPhysChem 19 (2018) 1781.

[31] T. Nguyen, V. Van, C. Gutlé, W. Stahl, M. Schwell, I. Kleiner, H. V. L. Nguyen, J. Chem. Phys. 152 (2020) 134306.

[32] S. Khemissi, H. V. L. Nguyen, ChemPhysChem 21 (2020) 1682.

[33] K. P. Rajappan Nair, S. Herbers, J.-U. Grabow, A. Lesarri, J. Mol. Spectrosc. 349 (2018) 37.

[34] K. P. Rajappan Nair, S. Herbers, D. A. Obenchain, J.-U. Grabow, A. Lesarri, J. Mol. Spectrosc. 344 (2018) 21.

[35] K. P. Rajappan Nair, D. Wachsmuth, J.-U. Grabow, A. Lesarri, J. Mol. Spectrosc. 337 (2017) 46.

[36] K. P. Rajappan Nair, S. Herbers, D. A. Obenchain, J.-U. Grabow, Can. J. Phys. 98 (2020) 543.

[37] S. Grimme, S. Ehrlich, L. Goerig, J. Comp. Chem. 32 (2011) 1456.

[38] H.V.L. Nguyen, J. Mol. Struct. 1208 (2020) 127909.

[39] J. R. Aviles-Moreno, J. Demaison, T. R. Huet, J. Am. Chem. Soc. 128 (2006) 10467.

[40] C. Pérez, M. T. Muckle, D. P. Zaleski, N. A. Seifert, B. Temelso, G. C. Shields, Z. Kisiel, B. H. Pate, Science 336 (2012) 897.

[41] H. V. L. Nguyen, R. Kannengießer, W. Stahl, Phys. Chem. Chem. Phys. 14 (2012) 11753.

[42] K. J. Koziol, W. Stahl, H. V. L. Nguyen, J. Chem. Phys. 153 (2020) 184308.

[43] H. V. L. Nguyen, J.-U. Grabow, ChemPhysChem 21 (2020) 1243.

[44] Z. Kisiel, O. Desyatnyk, L. Pszczółkowski, S. B. Charnley, P. Ehrenfreund, J. Mol. Spectrosc. 217 (2003) 115.

[45] L. Ferres, W. Stahl, H. V. L. Nguyen, Mol. Phys. 114 (2016) 2788.

[46] H. B. Schlegel, J. Comput. Chem. **3**, 214‑218 (1982).

[47] J.-U. Grabow, W. Stahl, and H. Dreizler, Rev. Sci. Instrum. 67 (1996) 4072.

[48] J.-U. Grabow, W. Stahl, Z. Naturforsch. 45a (1990) 1043.

[49] H. Hartwig, H. Dreizler, Z. Naturforsch. 51a (1996) 923.

[50] S. Herbers, S. M. Fritz, P. Mishra, H. V. L. Nguyen, T. S. Zwier, J. Chem. Phys. 152 (2020) 074301.